Original Paper

Hydrous sodium silicate glasses obtained by drying sodium silicate solutions

Hans Roggendorf and Dorit Böschel

Institut für Werkstoffwissenschaft, Martin-Luther-Universität Halle-Wittenberg, Halle (Germany)

Concentrated sodium silicate solutions with a SiO_2:Na_2O molar ratio of 3.3 and a SiO_2 content of 27 wt% were dried at temperatures between 30 and 100 °C to residual water contents between 11 and 45 wt%. The materials are brittle, transparent and X-ray amorphous. Their structure is discussed, with the conclusion that it is vitreous. The materials were investigated by thermal analysis techniques (e.g. differential scanning calorimetry in open and closed crucibles, thermogravimetry, hot stage microscopy), optical and electron microscopy, and X-ray diffraction. Up to six thermal events detected by thermal analysis are discussed. Two of these thermal events were analysed with respect to their heat rate dependence and are discussed with respect to structural transitions (glass to gel and gel to sol). Other events are also discussed, such as the temperatures of foam formation during heating and the boiling temperatures of the investigated samples.

1. Introduction

Alkaline silicate glasses and the solutions produced by dissolving the glasses are basic products of the chemical industry. An introduction to the field is given by Dent Glasser [1]. Sodium silicate solutions produced on an industrial scale are characterized by molar SiO_2:Na_2O ratios between 1.8 and 3.8 (ratios of 2.0 and 3.3 are standard compositions) and SiO_2 contents up to 30 wt% SiO_2. In some cases water is evaporated to adjust the concentrations. The solutions are used in the paper industry, for producing detergents, and as raw materials for silicate synthesis. For some applications the materials have to be dried. Spray-dried powders with a water content of about 10 to 20 wt% are sold as rapidly dissolvable silicates. Transparent layers of dried sodium silicate solutions (possibly containing some additives) are used in fire protection glazings. A fibre drawing technology based on drying sodium silicate solutions was developed by Achtsnit [2]. In the following, water-containing sodium silicates obtained by drying solutions are called hydrous sodium silicates.

A concentrated sodium silicate solution can structurally be described as a dispersion of colloidal amorphous silicates in an aqueous solution [3]. The solutions have pH values between 11 and 12 and are supposed to be saturated with silica at molecular level. The molecular chemistry of the solutions is described by Iler [4]. Quantitative ^{29}Si-NMR data concerning the structural surroundings of silicon in concentrated sodium silicate solutions were reported by Harris et al. [5]. The sizes of the colloids reported in the literature differ. Many publications report sizes between 1 and 5 nm. Iler [6], for instance, extracted the colloids with tetrahydrofuran and measured colloid sizes of 2 nm by ultrafiltration. Own measurements of concentrated solutions by dynamic light scattering yielded values between 30 and 100 nm [3].

During drying the viscosity of the solution raises as a function of the water content. This was described by Vail [7], who found that viscosity raises within a narrow concentration range by a few orders of magnitude.

Dent Glasser and Lee [8] investigated the drying process of sodium silicate solutions with a SiO_2:Na_2O molar ratio of 3.42 and a SiO_2 content of 29 wt% by thermal analysis and leaching of the dried products. In a two-step drying process they obtained hydrous sodium silicates with water contents between 10 and 37 wt%. The materials were investigated by thermogravimetric and differential thermal analysis in separate runs. Two endothermic events were detected: the lower temperature effect was explained by the rearrangement of interstitial ions and water molecules, whereas the higher tempera-

Received 27 September 2001, revised manuscript 24 January 2002.

ture effect was attributed to the evaporation of H_2O which is formed by the condensation of silanol groups.

Another type of hydrous sodium silicates was discussed from a different point of view. It is possible to melt crystalline sodium metasilicate hydrates (e.g. $Na_2O{\cdot}SiO_2{\cdot}nH_2O$, n=5, 6 and 9) and to solidify them in the vitreous state by cooling to low temperatures [9].

The glass transition of the above mentioned hydrous metasilicate glasses was investigated by unconventional methods. Scholze et al. [10] dried the melts to n-values between 2.6 and 4. They measured the vapour pressure above the dried materials in the temperature range of the glass transition. An unsteadiness of $\partial p(H_2O)/\partial T$ was attributed to the glass transition. Koller et al. [11] determined the glass transition of materials with n-values between 4 and 9 via the peak shapes in ^{29}Si MAS NMR spectra (MAS: magic angle spinning; NMR: nuclear magnetic resonance). Glass transition temperatures of −17 °C [10] and −11 °C [11], respectively, were determined for the hydrous silicate $Na_2O{\cdot}SiO_2{\cdot}4H_2O$, which is a good agreement for two different methods. Koller et al. distinguished three temperature regions with respect to the structural evolution: a glassy region (A, including the temperature of glass transformation) at the lowest temperatures, an aggregation region (B) at intermediate temperatures, in which the increase of viscosity during cooling is attributed to a growing degree of aggregation of polymeric silicate anions and a solution or electrolyte region (C) at higher temperatures. The structure of the glasses in temperature region A was described on the basis of a continuous polymeric network. The respective solutions were described as molecular solutions without colloids.

Modified hydrous sodium silicates obtained by drying sodium silicate solutions are used as fire protection materials. In the case of application (fire on one side of the glazing) these materials inhibit heat transfer by two processes. The first is the absorption of infrared radiation due to their water content. The second is the formation of a porous layer by a foaming process at temperatures between 120 and 200 °C. Foaming requires a deformable phase. Therefore, a solid/liquid transition is supposed to occur in the described application case.

Reactions like foaming interfere with conventional characterization methods, which may be one of the reasons for a lack of information concerning the scientific basis of the foaming process. To improve this situation, dried sodium silicate solutions were investigated by different means. Some results are already published, e.g. the method of thermal analysis under hydrothermal conditions [12], structural investigations by electron microscopy [13 and 14], and the method of hot stage microscopy [14]. In the following, further results obtained by applying these and other methods to a broader materials basis are presented.

2. Experimental

Technical-grade sodium silicate solutions (Roth, Karlsruhe (Germany)) were used as raw materials. The concentrations of the main components of the starting materials were determined chemically: e.g. 8.6 wt% Na_2O (by titration) and 27.3 wt% SiO_2 (gravimetrically; SiO_2:Na_2O molar ratio of 3.27). The solutions (between 5 and 15 g) were dried in open polypropylene beakers with a volume of 120 ml. The beakers were placed in closed drying ovens above a desiccant. After drying, the beakers were closed with a lid and stored for further 24 h at the drying temperature in order to minimize concentration gradients due to the diffusion of water. The weight loss of the sodium silicate solutions was measured and was used to calculate the residual water content. After drying and between the investigations the samples were stored in a desiccator.

The dried materials were examined by optical microscopy (Jenapol u, Carl Zeiss, Jena) and X-ray diffraction (Seifert ID 3000 with goniometer URD 63; Seifert, Freiberg (Germany)). By this means crystallized or cracked samples were identified. The diffraction pattern was usually recorded between 5° and 60° 2θ (CuK_α radiation) in the region of the glass halo. In some cases the recording range was extended to 100° 2θ.

The density of some of the dried materials was measured by applying Archimedes' principle.

Thermal analysis was performed with a Simultaneous Thermal Analyser (Netzsch STA 409 C; Netzsch, Freiberg (Germany)). The dried hydrous silicates were crushed to a particle size of about 100 µm. The samples were heated in a DSC-furnace (DSC = differential scanning calorimetry) up to 350 °C with a heating rate of 10 K/min. The following crucibles were used:

a) Open crucibles for the analysis at ambient pressure. For DSC measurements aluminium crucibles (sample mass 20 mg) were applied, covered by a lid kept open by a small hole. The hole was kept small in order to minimize evaporation. For calibration pure water (ion-exchanged) was analysed under the same conditions. An empty aluminium crucible was used as reference. The mass loss due to evaporation was recorded simultaneously. Larger samples (sample mass 100 mg) were analysed by DTA (differential thermal analysis) in alumina crucibles.

b) Closed crucibles: Evaporation is accompanied by weight loss and interferes with conventional DSC methods, e.g. to demonstrate a glass transition. Therefore, pressure-tight crucibles were applied to suppress evaporation. Closed aluminium crucibles can be applied for internal pressures up to 3 bar. With these crucibles the evaporation reactions can be suppressed up to about 140 °C. An empty aluminium crucible was used as reference. For higher pressures, closed autoclave crucibles (Netzsch) with 27 µl volume were used for measurements. Their application range is limited to 300 or

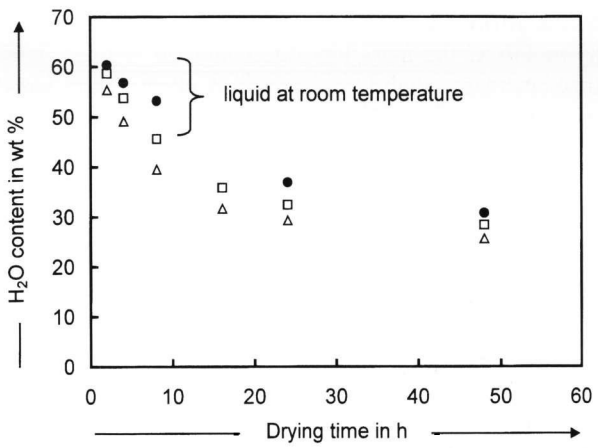

Figure 1. Drying of hydrous sodium silicates as a function of time; drying temperatures: •: 40 °C, □: 50 °C, Δ: 60 °C; SiO_2:Na_2O molar ratio = 3.27.

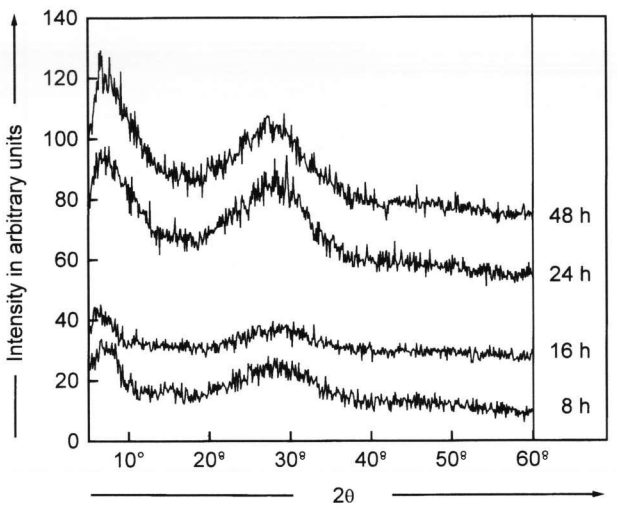

Figure 2. X-ray diffraction graphs of hydrous sodium silicates dried at 40 °C for different drying times; SiO_2:Na_2O molar ratio = 3.27.

350 °C in the case of aqueous systems (hydrous sodium silicates have a lower water vapour pressure than pure water). The crucibles (mass: 900 mg) were filled with 12 to 20 mg of the crushed samples. Pure water in an autoclave crucible was used as reference. Details of this technique are published in [12].

A hot stage microscope (Jenapol u, Carl Zeiss Jena, combined with the hot stage Mettler FP 84 HT) was used to monitor the structural changes of some samples of hydrous sodium silicates during heating. The hot stage microscope does not allow to measure weight changes due to evaporation. Therefore, in two cases a possible water loss during heating was controlled by heating identical samples in the DTA mode combined with thermogravimetry (TG) of the thermal analyser (Netzsch STA 409). Details of this method are reported in [14].

3. Results

3.1 Drying

Sodium silicate solutions dried by the above-described process solidified within the first 24 h, when the water content fell below 50 wt%. Usually, the resulting materials were transparent and brittle. The gravimetric results of the drying process were mainly used to calculate the actual water content of the samples. A typical graph showing the mass change of hydrous sodium silicates during drying is shown figure 1. It indicates a continuous drying process.

At temperatures ≤ 60 °C, the samples crystallized at water contents between 20 and 30 wt%. In the latter case, small amounts of crystals (< 5 wt%) were observed in optical microscopy and identified by X-ray diffraction as sodium carbonate. Usually, the samples were dried in normal atmosphere. In a separate set of drying experiments, the CO_2 access was inhibited. In these runs no crystallization was observed.

Above 60 °C cracks developed, probably due to mechanical stresses induced by concentration gradients. At these temperatures water contents down to 11 wt% were reached. The drying conditions (type of furnace, position in the furnace, geometry of the beaker, air humidity, etc.) have a great influence on the drying kinetics, e.g. [15]. Drying is regarded here as an evaporation process. These influences are at least partly responsible for differences of water contents between samples dried under identical time and temperature conditions.

3.2 X-ray characterization

Crystallization and cracking of the samples were distinguished by optical microscopy (see section 3.1). Diffraction patterns of the solid and transparent materials are shown in figure 2. These diagrams demonstrate the absence of crystals and the development of the typical diffraction halo of amorphous materials with increasing drying time.

3.3 Density

The densities of hydrous sodium silicates are shown in figure 3 as a function of the residual water content. The samples were dried first at 40 °C (first density measurement). Aliquots of these materials were dried further at 60 °C (second density measurement). Both data sets can be approximated by a linear relationship between density

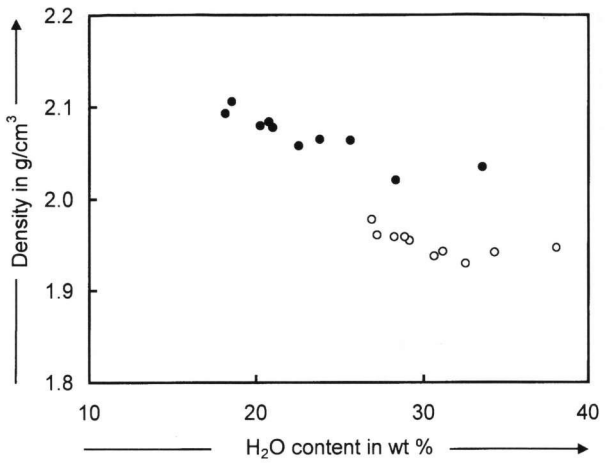

Figure 3. Density of hydrous sodium silicates as a function of the H_2O content for different drying temperatures: ○: 40 °C; •: first 40, then 60 °C; SiO_2:Na_2O molar ratio = 3.27.

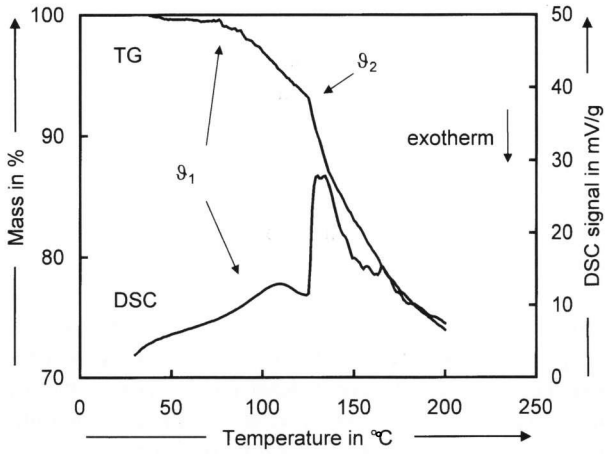

Figure 4. DSC and TG graphs of a hydrous sodium silicate with a H_2O content of 46.3 wt%; SiO_2:Na_2O molar ratio = 3.27; drying temperature = 40 °C; drying time = 16 h; open aluminium crucible; the discussed effects are indicated; the mass of the sample is referred to the initial mass (= 100 %).

and residual water content. Samples having the same residual water content but dried at 60 °C have a higher density than those dried only at 40 °C. This indicates the dependence of the structure of the amorphous hydrous sodium silicates on the drying conditions.

3.4 Thermal analysis

3.4.1 Open aluminium crucibles

Hydrous sodium silicates with water contents between 35 and 45 wt% and a drying temperature of 40 °C were analysed in open aluminium crucibles by DSC and TG. Typical graphs are shown in figure 4. The observed mass loss is attributed to the evaporation of water. At about 80 to 110 °C the mass loss rate $\partial m/\partial t$ (m = mass, t = time) increases slightly (discussed as effect 1, the temperature is named ϑ_1). This faint effect is accompanied by a DSC step, which is not easy to evaluate, due to the effects of evaporation and boiling. The temperature values of ϑ_1 are listed table 1.

At about 110 to 140 °C (effect 2 at ϑ_2) a further, significant change of the mass loss rate occurs. Due to the evaporation the composition of the samples changes gradually during the measurement. Hence, the original water content of the investigated samples at the start of the analysis had to be corrected to obtain the actual composition at the time of the actual point of measurement. The corrected temperature and composition data as well as the corresponding ϑ_2 values are listed in table 1. For comparison, pure water was analysed under the same conditions. At 102 °C an unsteadiness of the second derivative of the mass as a function of time was observed and at 118 °C an unsteadiness of the first derivative.

Additionally, two endothermic DSC peaks were observed (figure 4). The lower one at temperatures between 106 and 120 °C, the upper one at 125 to 145 °C.

3.4.2 Closed aluminium crucibles

The same set of materials with water contents between 35 and 45 wt% was analysed in closed aluminium crucibles too. A typical DSC and TG graph is shown in figure 5.

Between room temperature and about 140 °C no weight loss was observed. Additionally, no typical caloric events – neither endo- nor exothermic – were detected in that temperature range. At about 140 °C the aluminium crucibles burst, as indicated by a sudden, significant weight loss. The subsequent weight loss was accompanied by endothermic peaks.

Samples dried at temperatures above 60 °C and containing less water showed a DSC step with characteristics of a glass transition (effect 3 at ϑ_3). In a set of experiments the heating rate dependence of this thermal event was demonstrated (figure 6) for a sample dried for 3 d at 70 °C to a water content of 21.8 wt%. As characteristic temperatures the mid points of the Δc_p steps were evaluated. These temperatures increased from 56 °C (heating rate of 3 K/min) to 59 °C (5 K/min), 63 °C (10 K/min) and 69 °C (15 K/min) with the heating rate, which is also typical of glass transition.

3.4.3 Autoclave crucible

Thermal analysis with autoclave crucibles was carried out at temperatures up to 350 °C. Below 80 °C the evalu-

Table 1. Drying parameters, H_2O contents (after drying, corrected for the actual temperature at the determined effect) and temperatures of ϑ_1 and ϑ_2 of hydrous sodium silicates analysed in open aluminium crucibles; SiO_2:Na_2O molar ratio = 3.27; n.d.: not detected

drying temperature in °C	drying time in d	H_2O content in wt% (after drying)	H_2O content in wt% (at ϑ_1)	ϑ_1 in °C	H_2O content in wt% (at ϑ_2)	ϑ_2 in °C
40	0.67	46.3	44.9	88	42.0	122
40	0.33	43.6	n.d.	n.d.	41.2	120
40	0.33	43.6	n.d.	n.d.	39.4	120
40	1	42.9	41.8	90	38.0	130
50	1	38.9	37.5	102	34.3	128
40	1	37.8	36.5	97	33.1	128
60	2	36.2	35.2	103	n.d.	n.d.

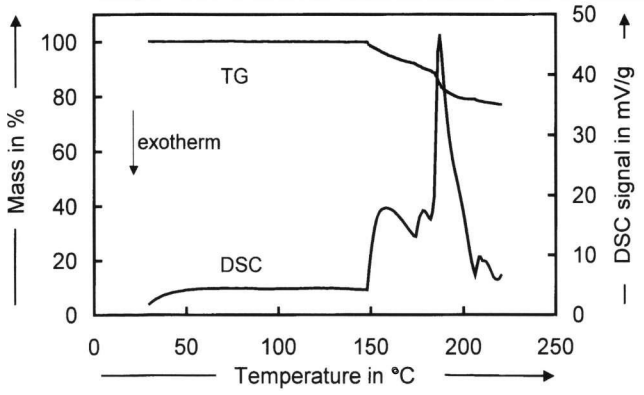

Figure 5. DSC and TG graphs of a hydrous sodium silicate with a H_2O content of 38.9 wt%; SiO_2:Na_2O molar ratio = 3.27; drying temperature = 50 °C; drying time = 24 h; closed aluminium crucible; the mass of the sample is referred to the initial mass (= 100 %).

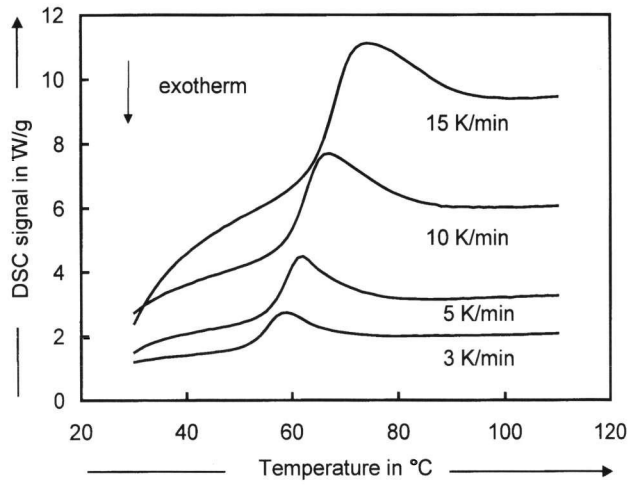

Figure 6. DSC graphs of a hydrous sodium silicate with a H_2O content of 21.8 wt% for different heating rates; SiO_2:Na_2O molar ratio = 3.27; drying temperature = 70 °C; drying time = 3 d; closed aluminium crucible.

ation of the DSC signal was difficult. This is due to the higher thermal mass of the stainless steel container. No distinct DSC peaks were observed in the DSC graphs, unless in cases of leaky crucibles. Most of the DSC curves revealed Δc_p steps resembling the DSC behaviour of a glass transition. Again the mid points of these steps were evaluated. The numerical results are listed in table 2. Two different types of DSC steps were identified. The low temperature effect is discussed as effect 4 (at ϑ_4) and the high temperature effect as effect 5 (at ϑ_5). The two types of DSC steps can be distinguished by their shape: effect 4 has a larger step height (Δc_p) than effect 5 but covers a smaller temperature range (ΔT) (as discussed in [12]). The temperatures of both effects depend on the water content, as shown in figure 7. The values of ϑ_5 are scattered over a broad temperature range. On the other hand, the data of samples originating from the same charge are reproducible (see data in table 2). The scattering is probably due to differences in the drying parameters. This corresponds to the findings of the density measurements (see section 3.3). The heating rate dependence of effect 5 cannot be easily interpreted. For a hydrous sodium silicate with 14.5 wt% H_2O the following values of ϑ_5 (mid points) were measured: 233 °C (heating rate 3 K/min), 229 °C (heating rate 5 K/min), 235 °C (heating rate 10 K/min), and 239 °C (heating rate 15 K/min). A hydrous sodium silicate with 22.4 wt% H_2O

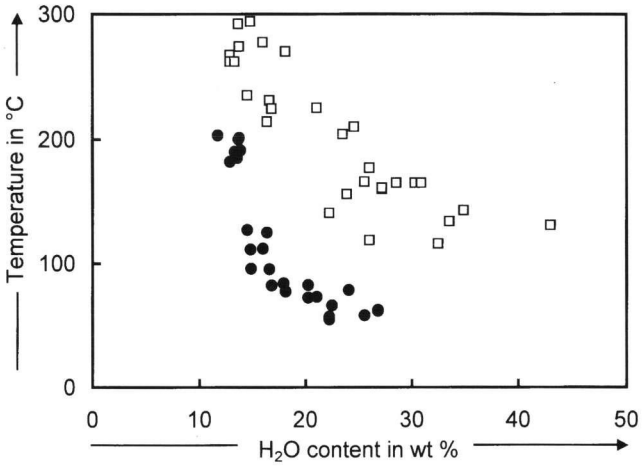

Figure 7. Mid point temperatures ϑ_4 (•) and ϑ_5 (□) of DSC steps measured in autoclave crucibles as a function of the H_2O content; SiO_2:Na_2O molar ratio = 3.27; samples characterized in table 3.

Table 2. Drying parameters, H_2O content and temperatures of ϑ_4 and ϑ_5 of hydrous sodium silicates analysed in autoclave crucibles; SiO_2:Na_2O molar ratio = 3.27; * indicates a second measurement with another sample of the same charge; drying temperature 100/50 °C and drying time 16 + 61 d means that the sample was first dried 16 d at 100 °C and then 61 d at 50 °C; n.d.: not detected

drying temperature in °C	drying time in d	H_2O content in wt% (after drying)	ϑ_4 in °C	ϑ_5 in °C
70	71	11.7	203	n.d.
100	64	12.9	182	267
100	64*	12.9	182	262
80	43	13.3	190	262
80	43*	13.3	190	262
80	88	13.6	185	n.d.
100	23	13.7	200	292
90	43	13.8	201	274
90	43*	13.8	201	274
80	64	13.9	191	n.d.
100/50	16 + 61	14.5	127	235
100	9	14.8	111	294
80	30	14.9	96	n.d.
100	16	16.0	112	277
70	28	16.4	125	214
100	4	16.6	95	231
70	24	16.8	82	224
80	4	17.9	84	n.d.
70	14	18.1	77	n.d.
40/60	26 + 23	18.1	n.d.	270
70	6	20.2	83	n.d.
70	6	20.2*	72	n.d.

yielded 125 °C (heating rate 3 K/min) and 141 °C (heating rate 10 K/min).

The values of ϑ_4 do not scatter to the same degree. The gap observed at a water content of 14 wt% cannot be explained at the moment. Effect 4 was observed only in samples with water contents < 26 wt%, which is probably due to the restrictions of the measurement range at lower temperatures. In many cases, both effects 4 and 5 were observed.

3.4.4 Hot stage microscopy

Several samples were investigated as solid compacts by hot stage microscopy. The foaming of the sample was observed. After foaming, the materials solidify again.

The foaming temperatures are listed in table 3. They are shown in figure 8 as a function of the water content and are discussed as effect 6 (at ϑ_6). The boiling temperatures measured with open aluminium crucibles (see section 3.4.1) are included for comparison.

Table 3. Drying parameters, H_2O content and temperatures of ϑ_6 (foaming) of hydrous sodium silicates analysed in the hot stage microscope; SiO_2:Na_2O molar ratio = 3.27; drying temperature 100/50 °C and drying time 16 + 61 d means that the sample was first dried 16 d at 100 °C and then 61 d at 50 °C

drying temperature in °C	drying time in d	H_2O content in wt% (after drying)	ϑ_6 in °C
100/50	16 + 61	14.5	161
60	2	21.6	147
60	1	23.5	130
60	2	27.1	150
60	0.67	29.5	141
60	1	32.0	130
50	1	37.1	150
60	0.29	42.7	112

3.5 Summary of experimental results

Concerning the structural evolution, the following results can be compiled:

- By drying the solutions to water contents between 45 and 11 wt% transparent, non-crystalline, X-ray amorphous and brittle materials can be obtained if crystallization and cracking is avoided.
- The materials foam upon heating.
- The foaming, which is a macroscopic solid/liquid transition, was observed in hot stage microscopy. After foaming the materials solidify again.
- In a first drying stage, structural units with sizes between 30 and 100 nm can be detected.
- Two different thermal events were observed, which show typical features of glass transition in thermal analysis.
- In many cases both effects (2 and 3) were observed.

To allow a structural discussion the structural findings reported in [14] are summarized in the following

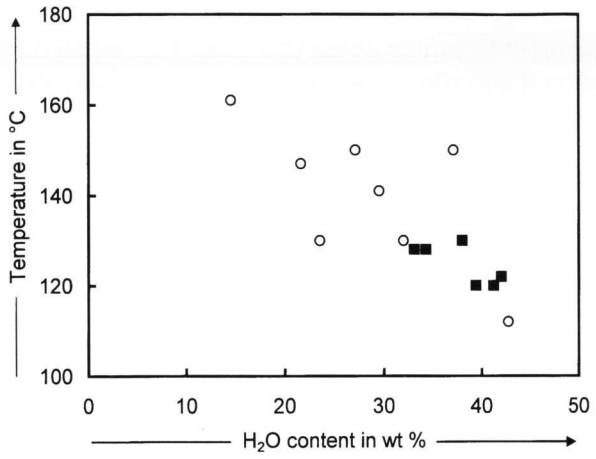

Figure 8. Temperature of foam formation ϑ_6 (o) and ϑ_2 (■) as a function of the H_2O content; SiO_2:Na_2O molar ratio = 3.27; samples characterized in tables 1 and 3.

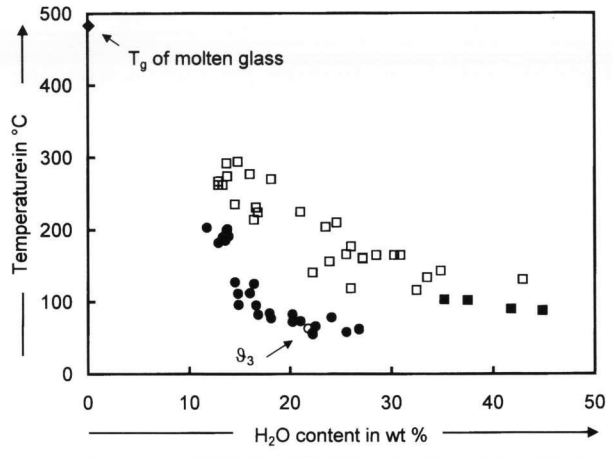

Figure 9. Comparison of the temperatures of thermal effects; ϑ_1 (■; data in table 1), ϑ_3 (o; heating rate 10 K/min, figure 6), ϑ_4 (•; data in table 2), ϑ_5 (□; data in table 2) as a function of the H_2O content; the glass transition temperature (◆) of a molten glass having the same SiO_2:Na_2O molar ratio = 3.27 and a water content of 0.1 wt% is included.

way: Samples dried at low temperature for short times (H_2O content > 30 wt%) have a particulate structure with a size range between 30 and 100 nm. The analysis suggests a smaller substructure. In samples dried more severely (H_2O content < 25 wt%), no particulate structure in the above reported size range was found.

4. Discussion

4.1 Thermal effects

Six thermal effects have to be discussed:

a) First change of mass loss rate in open crucible. As this change is observed below 100 °C, boiling is excluded as cause.

b) Second change of mass loss rate. An extrapolation to the composition of pure water leads to the conclusion that this effect is due to the boiling of the solutions. The measurement performed with pure water needs some discussion. It was possible to observe a slight change of the second derivative of the mass loss versus time near 100 °C, exactly at 102 °C. The change of the mass loss rate is influenced by the actual vapour pressure and the heat transfer from furnace to sample. The first derivative $\partial p/\partial T$ of the vapour pressure has no unsteadiness at the boiling point. Instead the temperature difference between sample and reference increases. This is possibly noticed as an effect of the second derivative of mass versus temperature. In the case of hydrous sodium silicates the highly viscous or even elastic state of the materials forbids materials transport by convection. The unsteadiness is thus possibly due to the formation of bubbles inside the materials which emerge and crack at the surface.

c) Transition temperature identified by a change of heat capacity in closed aluminium crucibles. A comparison with the results of electron microscopy [14] leads to the conclusion that effect 3 is due to the transition of the more homogeneous structure to the coarser particulate structure. The appearance of the Δc_p step and the heating rate dependence resemble a glass transition.

d) Low temperature transition identified in autoclave crucibles.

e) High temperature transition identified in autoclave crucibles by a change of heat capacity. One possible structural explanation might be a transition of the particulate structure to a free flowing solvent. The Δc_p step is smaller than for effect 3 or 4.

f) Foaming temperature. At this temperature the vapour pressure exceeds the ambient pressure. A comparison of foaming temperature and boiling temperature shows that the foaming temperature and the boiling temperature coincide. The foaming temperatures are measured in the temperature interval between effects 4 and 5. A vapour pressure slightly above 0.1 MPa is strong enough to deform the particulate structure. The mechanical properties of the materials between both temperatures must allow plastic deformation. It is concluded that the bonding between these particles or aggregates is not very strong.

In figure 9 the characteristic temperatures ϑ_1, ϑ_3, ϑ_4, and ϑ_5, respectively, and the T_g value measured for a melted glass with the same SiO_2:Na_2O molar ratio (water content below 0.1 wt%) are compared. The comparison suggests that effects 1 and 5 have the same cause. The same can be said with respect to effects 3 and 4, even if only one temperature point of effect 3 can be shown. This leaves four different thermal effects:

- boiling temperature,
- foaming temperature, and
- two different transition effects.

4.2 Structure of hydrous sodium silicates

There are several ways to define the vitreous state. Traditionally, glasses are defined as "fusion products of inorganic materials which have been cooled to a rigid condition without crystallizing" [16]. Today, the definition has to cover a wider range of materials (polymers, metals) and preparation processes [17]. Mackenzie [18] defined that all solid amorphous materials are glasses, whereas Zarzycki [17] demanded the demonstration of a glass transition, usually by thermal analysis.

Dried sodium silicates with a water content of less than 45 wt% are transparent, non-crystalline, X-ray amorphous and brittle materials. According to [17] they can be recognized as vitreous materials, if the application of X-ray diffraction and optical microscopy is regarded as a sufficient tool to demonstrate the amorphous structure.

The appearance of the investigated materials after thermal treatment as well as the hot stage microscopy indicate a macroscopic transition from a solid to a plastically deformable state.

The shapes of the observed Δc_p steps fit to a glass transition. A heating rate dependence typical of glass transitions was demonstrated for effect 3. Both effects, 4 as well as 5, were observed in the same DSC run in autoclave crucibles with hydrous sodium silicates containing less than 26 wt% H_2O. At higher water contents, either the temperature of effect 4 is too low to be seen in the autoclave crucibles or the temperature of effect 5 is too high to be observed in closed aluminium crucibles with the applied equipment. The following structural sequence is therefore proposed for hydrous sodium silicates with low water contents (< 26 wt%):

- From room temperature to ϑ_4: amorphous solid materials with a homogeneous or small scale (< 10 nm) structure.
- From ϑ_4 to ϑ_5: Solid aggregate structure which can be deformed by weak forces. Since this structure has similarities to a gel state, aggregates connected to a room filling network with a solution phase in the voids, ϑ_5 might be interpreted as a reversible sol/gel transition.
- Above ϑ_5: free flowing liquid.

Regarding this sequence, neither effect 4 nor effect 5 are glass transitions in the classical sense. However, effect 4 might be regarded as a glass transition superimposed by a rearrangement of the "melt" to a gel structure.

With respect to length scales, the greater height of the Δc_p step of effect 4 indicates that the structural units responsible for such a transition are smaller than those responsible for the Δc_p step of effect 5. This corresponds to the results of electron microscopy [14].

From these findings a model of the structural changes during drying was developed, which is discussed in [14]. In short, the sol is dried to a gel, which is rearranged by further drying to a glass. That means that effect 4 and effect 5 are transitions which occur when the temperature or the composition is changed.

The solidification described in that model reminds of a sol/gel transition in a particulate sol. On the other hand, the high density of the hydrous sodium silicates indicates a rather dense packing of aggregates or colloids, which is sometimes called colloid glass [19]. So the solidification of sodium silicate solutions during drying might be discussed as an extreme case of sol/gel transition or as a sol/colloid glass transition. The high density of the hydrous sodium silicates fits better to a sol/colloid glass transition. On the other hand, it appears tricky to define the difference between a colloid glass and a gel with a dense packing of colloids.

4.3 Comparison with literature data

The ϑ_4 values coincide with the thermal effects measured by Dent Glasser et al. [8]. The discussion of this coincidence is rather difficult, since the authors did not correct the composition data with respect to evaporation losses during thermal analysis. Nevertheless, the comparison hints that the gap at 14 wt% H_2O content has a structural background.

A comparison with the results of Koller et al. [11] shows that both materials investigated have a similar temperature dependence of the structure. Heating the solid leads from a vitreous structure via a particulate or aggregate structure (which is liquid in the case described in [11]) to a solution structure. The remaining structural differences seem to be due to differences of chemical composition.

5. Summary

Transparent, solid and amorphous materials were obtained by drying sodium silicate solutions. The combined application of simultaneous thermal analysis, electron microscopy and hot stage microscopy helps to identify thermal reactions occurring upon heating these materials. One of these reactions can be described as a glass transition combined with a reaction. The demonstration of such a glass transition extends our knowledge of the structure of hydrous sodium silicates and explains their behaviour as fire protection materials. Drying sodium silicate solutions with a molar ratio of 3.3 was thus shown to be another unconventional method to make glasses.

A glass transition may also explain the behaviour of fire-protecting glazings based on hydrous sodium silicates: The transparent fire-protecting layer foams in the case of application and forms a porous thermal insu-

lation layer. Foaming occurs when the hydrous sodium silicate becomes deformable for the first time, that is at the point of glass transition. In the case of fire-protecting glazings the hydrous sodium silicates can expand without restraint until the water content of the glass is so low that it solidifies again.

*

The kind support of the electron microscopy team of Prof. Dr. G. H. Michler, and the experimental assistance of Mrs. S. Brinke, Mrs. H. Schwalbe, and Dr. J. Trempler (optical microscopy) is gratefully acknowledged.

6. References

[1] Dent Glasser, L. S.: Sodium silicates. Chem. Britain **18** (1982) p. 33–39.
[2] Achtsnit, H.-D.: Microporous silica fibres. In : Fricke, J. (ed.): Aerogels. Proc. 1st Int. Symp. Würzburg 1985. Berlin et al.: Springer, 1986. p. 76–81.
[3] Roggendorf, H.; Grond, W.; Hurbanic, M.: Structural characterization of concentrated alkaline silicate solutions by ^{29}Si-NMR spectroscopy, FT-IR spectroscopy, light scattering, and electron microscopy – molecules, colloids, and dissolution artefacts. Glastech. Ber. Glass Sci. Technol. **69** (1996) no. 7, p. 216–231.
[4] Iler, R. K. : The chemistry of silica. New York: Wiley, 1979.
[5] Harris, R. K.; Bahlmann, E. K. F; Metcalfe, K. et al.: Quantitative silicon 29 NMR investigations of highly-concentrated high-ratio sodium silicate solutions. Magn. Reson. Chem. **31** (1993) p. 743–747.
[6] Iler, R. K.: Colloidal components in solutions of sodium silicate. In: Falcone, J. S. (ed.): Soluble silicates. Washington, DC: Am. Chem. Soc., 1982. p. 95–114.
[7] Vail, J. G.: Soluble silicates – their properties and uses. Vol. 1: Chemistry. New York: Reinhold, 1952. p. 89. (Am. Chem. Soc. Monograph Series.)
[8] Dent Glasser, L. S.; Lee, C. K.: Drying of sodium silicate solutions. J. Appl. Biotechnol. **21** (1973) p. 127–133.
[9] Berthaud, E. F.: Compatibility of hydrated sodium metasilicate glasses with inorganic and organic compounds. J. Am. Ceram. Soc. **45**, (1962) p. 56–59.
[10] Scholze, H.; Gliemeroth, G.: Dampfdruckmessungen an $Na_2SiO_3 \cdot nH_2O$-Gläsern Glastechn. Ber. **39** (1966) no. 1, p. 11–14.
[11] Koller, H.; Engelhardt, G.; Felsche, J.: Variable temperature ^{1}H, ^{23}Na, and ^{29}Si MAS NMR studies on sodium silicate hydrates of composition $Na_2O \cdot SiO_2 \cdot nH_2O$ (n = 9, 6, 5): Local structrure in crystals, melts, supercooled melts and glasses. Z. Anorg. Allg. Chem. **621** (1995) p. 301–310.
[12] Roggendorf, H.; Böschel, D.; Rödicker, B.: Differential scanning calorimetry at hydrothermal conditions of amorphous materials prepared by drying sodium silicate solutions. J. Therm. Anal. Calor. **63** (2001) p. 641–652.
[13] Böschel, D.; Trempler, J.; Roggendorf, H.: Micro-structural characterization of non-crystalline solids obtained by drying sodium silicate solutions. Glastech. Ber. Glass Sci. Technol. **71C** (1998) p. 276–279.
[14] Roggendorf, H.; Böschel, D.; Trempler, J.: Structural evolution of sodium silicate solutions dried to amorphous solids. J. Non-Cryst. Sol. **293–295** (2001) p. 752–757.
[15] Conradt, R.; Scholze, H.: Zur Verdampfung aus Glasschmelzen. Glastechn. Ber. **59** (1986) p. 34–52.
[16] German standard DIN 1259, T.1 (1986): Glas, Begriffe für Glasarten und Glasgruppen. Berlin: Beuth, 1986.
[17] Zarzycki, J.: Les verres et l'etat vitreux. Paris: Masson, 1982.
[18] Mackenzie, J. D.: General aspects of the vitreous state. In: Mackenzie, J. D. (ed.): Modern aspects of the vitreous state. London: Butterworths, 1960. p. 1–9.
[19] Pusey, P. N.; VanMegen, W.: The glass transition of hard spherical colloids. Ber. Bunsenges. Phys. Chem. **94** (1990) p. 225–229.

E202P006

Contact:

Prof. Dr.-Ing. H. Roggendorf
Martin-Luther-Universität Halle-Wittenberg
D-06099 Halle (Saale)
E-mail: hans.roggendorf@iw.uni-halle.de